Nucleic Acids Research, 2006, Vol. 34, No. 2 ***e16***
doi:10.1093/nar/gnj014

Therapeutic protein transduction of mammalian cells and mice by nucleic acid-free lentiviral nanoparticles

Nils Link, Corinne Aubel[1], Jens M. Kelm, René R. Marty, David Greber, Valentin Djonov[2], Jean Bourhis[1], Wilfried Weber and Martin Fussenegger*

Institute for Chemical and Bio-Engineering (ICB), Swiss Federal Institute of Technology, ETH Hoenggerberg HCI F115, Wolfgang-Pauli-Strasse 10, CH-8093 Zurich, Switzerland, [1]Radiosensibilité des Tumeurs et Tissus Sains, Institut Gustave-Roussy, 39 Rue Camille Desmoulins, 94805 Villejuif Cedex, France and [2]Institute of Anatomy, University of Bern, Baltzerstrasse 2, CH-3009 Bern, Switzerland

Received November 18, 2005; Revised and Accepted January 11, 2006

ABSTRACT

The straightforward production and dose-controlled administration of protein therapeutics remain major challenges for the biopharmaceutical manufacturing and gene therapy communities. Transgenes linked to HIV-1-derived *vpr* and *pol*-based protease cleavage (PC) sequences were co-produced as chimeric fusion proteins in a lentivirus production setting, encapsidated and processed to fusion peptide-free native protein in pseudotyped lentivirions for intracellular delivery and therapeutic action in target cells. Devoid of viral genome sequences, protein-transducing nanoparticles (PTNs) enabled transient and dose-dependent delivery of therapeutic proteins at functional quantities into a variety of mammalian cells in the absence of host chromosome modifications. PTNs delivering *Manihot esculenta* linamarase into rodent or human, tumor cell lines and spheroids mediated hydrolysis of the innocuous natural prodrug linamarin to cyanide and resulted in efficient cell killing. Following linamarin injection into nude mice, linamarase-transducing nanoparticles impacted solid tumor development through the bystander effect of cyanide.

INTRODUCTION

Therapeutic interventions that complement molecular deficiencies through the application of protein pharmaceuticals are the cornerstone of modern medicine (1). While the biopharmaceutical manufacturing industry focuses on production and regular administration of protein therapeutics (1), the gene therapy community capitalizes on therapeutic transgene delivery for sustained reversion of genetic defects (2). Although several protein therapeutics have been clinically licensed, downstream processing, delivery and pharmacokinetics continue to be major scientific and economic challenges (1). Likewise for gene therapy, advances in designing efficient viral systems for chromosomal transgene integration (3), and progress in expression dosing (4) are overshadowed by safety concerns associated with inadvertent tumor formation resulting from unspecific integration into non-malignant cells as evidenced in the first human trials (2,5,6).

For transient delivery of therapeutic transgenes, pseudotransduction (7,8), non-viral transfection technologies (9) and episomal vectors (10) have been designed. Non-genetic approaches for therapeutic delivery include directly delivered therapeutic macromolecules using polymer- and liposome-based drug-delivery systems (8), and trojanic fusion peptides which transfer proteins into mammalian cells by an unknown energy- and receptor-independent mechanism (11).

With a global mortality rate of 12%, malignant tumors are amongst the most severe of human pathologies, and therefore cancer therapy continues to be a priority for biopharmaceutical manufacturing and gene therapy societies (1,12). A number of strategies have been developed in the past to sensitize tumor cells to specific prodrugs. One of the most successful approaches is the *Herpes simplex* thymidine kinase (HSVtk)—ganciclovir system in which HSVtk-mediated phosphorylation of nucleoside analogs, including ganciclovir, blocks DNA replication (13). Another technology is based upon the natural linamarase—linamarin prodrug system which has evolved as a defense mechanism against insect herbivores in Cassava (*Manihot esculenta*) plants (14). Damage of the Cassava cell walls by insect larvae releases

*To whom correspondence should be addressed. Tel: +41 44 6333448; Fax: +41 44 633 1234; Email: fussenegger@chem.ethz.ch
Present addresses: Jens M. Kelm, Institute for Tissue Engineering and Cell Transplantation, Zurich University Hospital, Raemistrasse 100, CH-8091 Zurich, Switzerland
René R. Marty, Research Department, Basel University Hospital, Hebelstrasse 20, CH-4031 Basel, Switzerland

the β-glucosidase linamarase which is stored in the plant cell vacuoles. Linamarase hydrolyses the extracellular innocuous cyanogenic glucoside substrate linamarin into glucose, acetone and gaseous cyanide thereby mediating efficient cell killing (15). As linamarin is not hydrolyzed by most mammalian tissues, it remains innocuous (LD_{50}, 300 mg/kg body weight) and is readily excreted through the urine (15–17).

We have combined classic transient transfection-based protein production with *in situ* encapsidation into engineered nucleic acid-free nanoparticles to enable transient and dose-controlled intracellular delivery of protein pharmaceuticals into mammalian cells and mice. This protein transduction technology combines the best features of biopharmaceutical manufacturing (e.g. ease of protein production) and gene therapy (e.g. efficient transduction) without sharing their major disadvantages, such as unpredictable pharmacokinetics and transgene-chromosome cross-talk resulting from random proviral integration.

MATERIALS AND METHODS

Vector design

The helper plasmid **pWW203** encoding a deficient integrase (D64E mutation) was constructed by PCR-mediated amplification of pCD/NL-BH* (18) (primers: OWW101: 5′-gtccaggaatatggcaactCgaGtgtacacatttagaagg-3′ and OWW102: 5′-ccttctaaatgtgtacaCtcGagttgccatattcctggac-3′; annealing sequence lowercase, mutations uppercase) using the QuikChange® kit (Stratagene, La Jolla, CA). **pWW240** ($P_{hEF1\alpha}$-VPR-PC-pA_{BGH}) contains a PCR-amplified HIV-1-derived VPR-PC (PC, *pol*-derived protease cleavage site) fusion peptide [primers: OWW120: 5′-GCGCGCCCAccatg-gaacaagccccagaag-3′ and OWW121: 5′-GCTAGCGtctt-gggccttatctattccatc-3′; template: pLR2P-R-PC-IN (7)] which was ligated in sense orientation into pEF6/V5-HIS-TOPO (Invitrogen, Carlsbad, CA). **pWW315** ($P_{hEF1\alpha}$-VPR-PC-LIS-HA-pA_{BGH}) was constructed by NheI/NotI-mediated in-frame cloning of the PCR-amplified [primers: OWW308: 5′-GCCTAGCTAGCatgctcgtcttgttcataagc-3′ and OWW309: 5′-ATAGTTTAGCGGCCGCCTAAGCGTAATCTGGAAC-ATCGTATGGGtacatcacatagaatttgccaacc-3′; template: pL*lis*SP (19)] and hemaglutinin A (HA)-tagged Cassava (*M.esculenta*) linamarase (LIS) 3′ of pWW240-encoded VPR-PC. **pWW326** ($P_{hEF1\alpha}$-VPR-PC-RIPDD-HIS-pA_{BGH}) was constructed by restricting PCR-amplified [primers: OWW310: 5′-GCCTAGCTAGCatggactacaaagacgatgacg and OWW319: 5′-GCTCTAGAGCAAGCTTTTAATGGT-GATGATGgttctggctgacgtaaatca-3′; template: pRIPDD (20)] and hexahistidine (HIS)-tagged human RIP death domain (RIPDD) with NheI (cuts RIPDD fragment 5′ while 3′ end remains blunt) and replacing LIS of pWW315 by RIPDD (NheI/EcoRV). **pNLK8** ($P_{hEF1\alpha}$-GFP-HIS-pA_{BGH}) was designed by SalI/MluI-mediated cloning of PCR-amplified green fluorescent protein (GFP) [primers: ONLK6: 5′-ACGCGTCGACGCTAGcatggtgagcaagggcga-gga-3′ and ONLK7: 5′-CGACGCGTGCAAGCTTGCGG-CCGCTTAATGGTGATGGTGATGATGcttgtacagctcgtccat-gcc-3′; template: pMF365 (21)] into the corresponding sites (SalI/MluI) of pBM43 (21). For construction of **pNLK9** ($P_{hEF1\alpha}$-VPR-PC-GFP-HIS-pA_{BGH}) GFP-HIS was excised from **pNLK8** by NheI/NotI and cloned into the corresponding sites (NheI/NotI) of pWW240. **pNLK11** ($P_{hEF1\alpha}$-VPR-PC-HSVtk-HA-pA_{BGH}) harbors PCR-amplified (primers: ONLK8: 5′-GCCTAGCTAGCatgcccacgctactgcgg-3′ and ONLK9: 5′-ATAGTTTAGCGGCCGCCTAAGCGTAAT-CTGGAACATCGTATGGGcagttagcctcccccatctc-3′; template: pWW204, W. Weber unpublished data) and HA-tagged HSVtk cloned 3′ in-frame (NheI/NotI) of pWW240-encoded VPR-PC.

Cell culture

Human embryonic kidney [HEK293-T; (21)], human breast adenocarcinoma (MCF7; ATCC HTB-22) and human fibrosarcoma (HT-1080; ATCC CCL-121) cells were cultivated in DMEM; Invitrogen supplemented with 10% heat-inactivated fetal calf serum (FCS) (PAN biotech GmbH; Aidenbach, Germany; Cat. No. 3302-P231902, Lot. No. P231902) at 37°C in a 5% CO_2-containing humidified atmosphere. Likewise, Chinese hamster ovary cells (CHO-K1; ATCC CCL-61) were cultivated in FCS-containing FMX-8 (Cell Culture Technologies GmbH; Lugano, Switzerland) and mouse mammary gland cells (4T1; ATCC CRL2935) in FCS- and L-glutamine (2 mM) supplemented RPMI 1640 medium. Tumor spheroids were generated by gravity-enforced self-assembly following cultivation of 1000 MCF7 or 3000 4T1 cells in hanging drops containing DMEM supplemented with 20% KnockOut Serum Replacement (Invitrogen; Cat. No. 10828-028) (22). For qualitative viability analysis of cells in entire tumor spheroids, the microtissues were washed twice in phosphate-buffered saline (PBS) and incubated for 5 min in ethidium bromide (0.0125% in H_2O)—fluorescein-diacetate (0.0005% in H_2O) solution before the spheroids were visualized by fluorescence microscopy (Leica DM-RB equipped with a DC300 FX camera; Leica Microsystems AG, Heerbrugg, Switzerland). Cell number and viability of cell suspensions generated from monolayers (5 min incubation in 0.5 ml prewarmed Trypsin/EDTA solution [PAN Biotech GmbH], addition of 2 ml DMEM) and spheroid cultures (pooling of 120 spheroids, 1× washing in PBS, 5 min incubation in 0.5 ml non-enzymatic cell dissociation solution [Sigma Chemicals] under rigorous shaking at 37°C, 5 min incubation in 0.5 ml prewarmed Trypsin/EDTA solution while pipetting up and down and addition of 5 ml DMEM) were quantified using a Casy1® cell counter (Schaerfe System GmbH, Reutlingen, Germany; Analyzer System Version 4.0).

Production of protein-transducing nanoparticles (PTNs)

PTNs were produced, quantified and characterized according to protocols established for small-scale lentivirus production (23). In brief, a DNA mixture containing (i) the vesicular stomatitis virus G protein-encoding pLTR-G (5 μg) for PTN pseudotyping, (ii) the helper construct pWW203 (5 μg) providing PTN assembly functions *in trans* and (iii) a product vector (10 μg) (e.g. pWW315, linamarase; pWW326, RIPDD; pNLK9, GFP; pNLK11, HSVtk) encoding the desired heterologous protein in an encapsidation-competent format (pNLK8, GFP as encapsidation-incompetent control) were transiently transfected into HEK293-T (2.5×10^6) (23). PTNs (typically 1×10^6 c.f.u.)

were collected from the culture supernatant (10 ml) 60 h after transfection by filtration (0.45 μm; Schleicher & Schuell GmbH, Dassel, Germany) and centrifuged for 3.5 h at 4°C (Beckman LM-8 ultracentrifuge, Ti50.2 rotor, 70 000 *g*, optiseal tubes; Beckman Instruments Inc., CA). The PTN pellet was resuspended in 600 μl FCS-supplemented DMEM for titer quantification (23) (p24-specific enzyme-linked immunosorbent assay (ELISA); Immunodiagnostics Inc., Bedford, MA), application or cryopreservation at −80°C. Following determination of viral p24 antigen, the quantity of viral particles was calculated as follows: The HIV-1 capsid consists of up to 2000 p24 proteins (MW = 25 550 g/mol) (24,25). Therefore, the viral quantity was calculated as particles [particles/ml] = p24 amount [μg/ml] × 1 × 10^{-6} × [Avogadro/(25 550 × 2000)]. Subsequently, the GFP content of the PTN batch was determined by western blot analysis. Specifically, varying amounts of both p24 (ranging from 1.8 to 0.06 μg) and a GFP-His standard (ranging from 0.6 to 0.03 μg) were loaded for PAGE. The intensity of western blot signals of PTN-packaged GFP was quantified by comparison with the GFP standard using a ChemiLux imager (Intas Science Imaging Instruments GmbH, Göttingen, Germany) with Gel-Pro Analyzer software installed (version 4.5; Media Cybernetics, Inc., Silver Spring, MD). The average ratio of GFP proteins per particle was then calculated from the quantified PTN and GFP concentrations.

Administration of PTNs, linamarin application, cyanide quantification and western blot analysis

Monolayer (T25 flask; TPP, Trasadingen, Switzerland; 3 × 10^5 cells) and spheroid (MicroWell MiniTray, Nunc GmbH, Wiesbaden, Germany; 1 spheroid [MCF7: 1000 cells/spheroid; 4T1: 3000 cells/spheroid]) cultures were typically transduced with PTNs at a MOI of 9. 24 h (48 h for 4T1) after seeding/aggregation cells were treated with linamarin (2-OH-isobutyronitrile-b-D-gluco-pyranoside; 750 μg/ml in H_2O, monolayers; 250 μg/ml H_2O, spheroids; TRC, Toronto, Canada) when indicated and the culture flask/plate was sealed airtight for 48 h to prevent HCN evaporation during cultivation. Samples were stored at −20°C and cyanide was quantified using a modified protocol described by Lambert and colleagues. In brief, solution A (oxidizing reagent) was prepared by sequential dissolution of 5 g succinimide and 0.5 g *N*-chlorosuccinimide in 300 ml H_2O with subsequent dilution to 500 ml using H_2O (storage at RT). Solution B was generated by dissolution of 0.6 g barbituric acid in 4 ml H_2O, addition of 3 ml pyridine and subsequent final dilution to 10 ml using H_2O. Solution B was aliquoted and stored at −20°C. Immediately prior to use, 6 ml of solution A was mixed with 120 μl of 1 M NaOH and 600 μl of 1 M acetic acid. To 224 μl of this mix was added 40 μl of culture medium sample and 40 μl amount of solution B. The combined mixture was vortexed and incubated for 10 min at room temperature after which 100 μl aliquots were transfered to a 96-well plate for spectrophotometric analysis. Cyanide concentration was determined by measuring absorption at 600 nm on a TECAN Genios PRO reader (Tecan AG, Maennedorf, Switzerland) which was calibrated using standardized sodium cyanide solutions (all chemicals from Sigma, St Louis, MO). Western blot analysis was performed as described previously (4) using HIS- and HA-specific antibodies (Novagen, Madison, WI and Santa Cruz Biotechnology, Santa Cruz, CA).

Animal experiments

Suspended 4T1 cells were adjusted in serum-free DMEM to 1.2 × 10^6 cells/ml and 100 μl was subcutaneously injected into female nude mice (Janvier CERT, Le Genest St Isle, France). After 6 days developed tumors (6 mm diameter) were measured using a sliding caliper before the mice were treated twice daily (8 a.m. and 5 p.m.) by sequential intratumoral injection of 1 × 10^{10} linamarase-transducing nanoparticles and 500 μg linamarin. Control mice received equal amounts linamarase-transducing nanoparticles, but H_2O instead of linamarin. After 4 days, mouse sera were analyzed for cyanide levels and tumor size was determined prior to removal. Each data point represents the average of at least 10 mice. All experiments involving animals were approved by the French Ministry of Agriculture and Fishery (C94-076-11) and performed at the Institute Gustave Roussy, Paris, France.

Histology

Explanted tumors were fixed in 2% formaldehyde—0.9% sodium chloride solution, washed twice in PBS and cryopreserved in 70% EtOH for histologic analysis. Tumor samples were embedded in paraffin and 3 μm slices generated by an Ultracut device (Zeiss, Feldbach, Switzerland). Slices were stained by haematoxylin/eosin and visualized by light microscopy. Semi-thin sections were obtained at a nominal thickness of 1 μm, stained with Toluidine blue, and viewed under a Vanox BHS light microscope (Olympus AG, Volketswil, Switzerland).

RESULTS

Design and characterization of PTNs

Production of protein-transducing lentiviral nanoparticles required transient cotransfection of three complementary plasmids into HEK293-T: (i) pLTR-G, which constitutively produces the vesicular stomatitis virus G protein for particle pseudotyping, (ii) pWW203, a helper plasmid which provides proteins essential for particle formation and (iii) a constitutive expression vector that encodes the protein of interest N-terminally linked to a fusion peptide consisting of VPR and the *pol*-derived 45 bp PC site which enables VPR-mediated packaging and viral protease-mediated VPR-PC release resulting in encapsidation of the native heterologous protein (Figure 1A). Following HEK293-T transfection with these plasmids, heterologous fusion protein was produced, processed and encapsidated into pseudotyped nucleic acid-free lentivirions which transduced the native protein into target cells (Figure 1B). Purified PTN samples were tested for potential residual carry-over of cytoplasmatic-derived transfected plasmid DNA by PCR analysis which confirmed that tested PTNs were nucleic acid-free (data not shown). VPR-PC-GFP produced in HEK293-T localized mainly at specific structures which are most likely particle assembly sites, while GFP

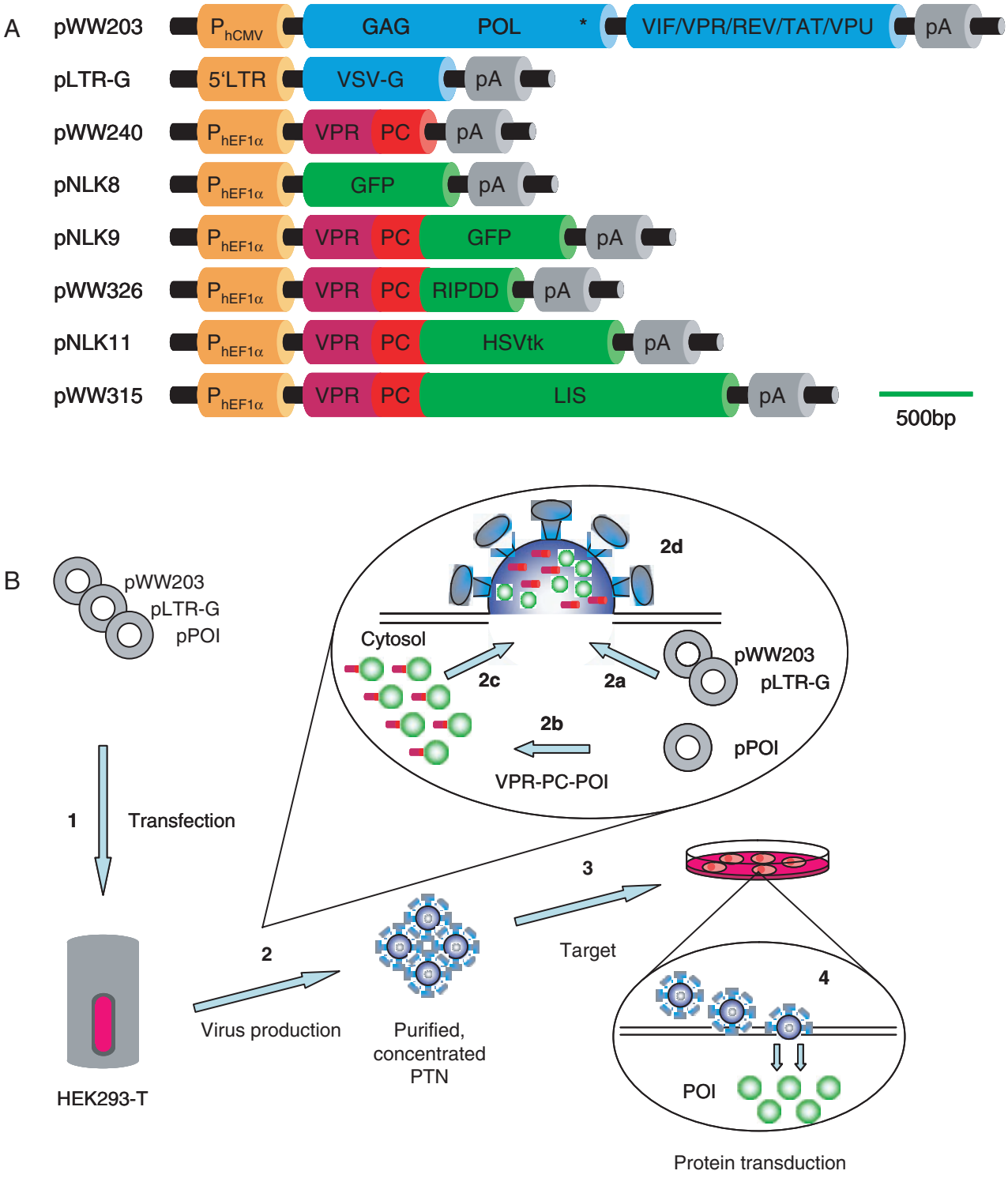

Figure 1. Molecular configuration of PTNs. (**A**) Schematic representation of expression vectors required for the protein transduction technology. Transgenes are drawn to scale. (**B**) Illustration of production and use of PTNs. (1) Transient cotransfection of (i) helper construct pWW203, (ii) pseudotyping vector pLTR-G, (iii) heterologous protein-encoding lentivector (pPOI) into the PTN production cell line HEK293-T. (2) While pWW203- and pLTR-G-encoded proteins mediated assembly of nucleic acid-free pseudotyped HIV-1-derived lentiviral nanoparticles (2a), the VPR-PC-tagged protein of interest (POI) was produced (2b) and targeted to the lentivirions (2c), where the VPR-PC tag was released by the *pol*-encoded viral protease and the native POI was encapsidated into budding PTNs (2d). (3) PTNs recovered from the culture supernatant were purified and concentrated by centrifugation and administered to target cells into which the POI was transduced (4). Abbreviations: 5′LTR, 5′ long terminal repeat; GAG, HIV-1 gene encoding core proteins; GFP, green fluorescent protein; HSVtk, *Herpex simplex* virus type 1 thymidine kinase; LIS, *Manihot esculenta* (Cassava) linamarase; pA, polyadenylation site; P_{hCMV}, human cytomegalovirus immediate early promoter; P_{hEF1a}, human elongation factor 1a promoter; RIPDD, RIP death domain—C-terminal domain of the human serine-threonine kinase 1 receptor; $POL^{(*)}$, gene encoding virion-associated enzymes including [*] integration-deficient integrase; VSV-G, vesicular stomatitis virus G protein; VIF/VPR/REV/TAT/VPU, HIV-1 accessory proteins; VPR, encapsidation-competent HIV-1-derived accessory protein; PC, *pol*-derived protease cleavage site.

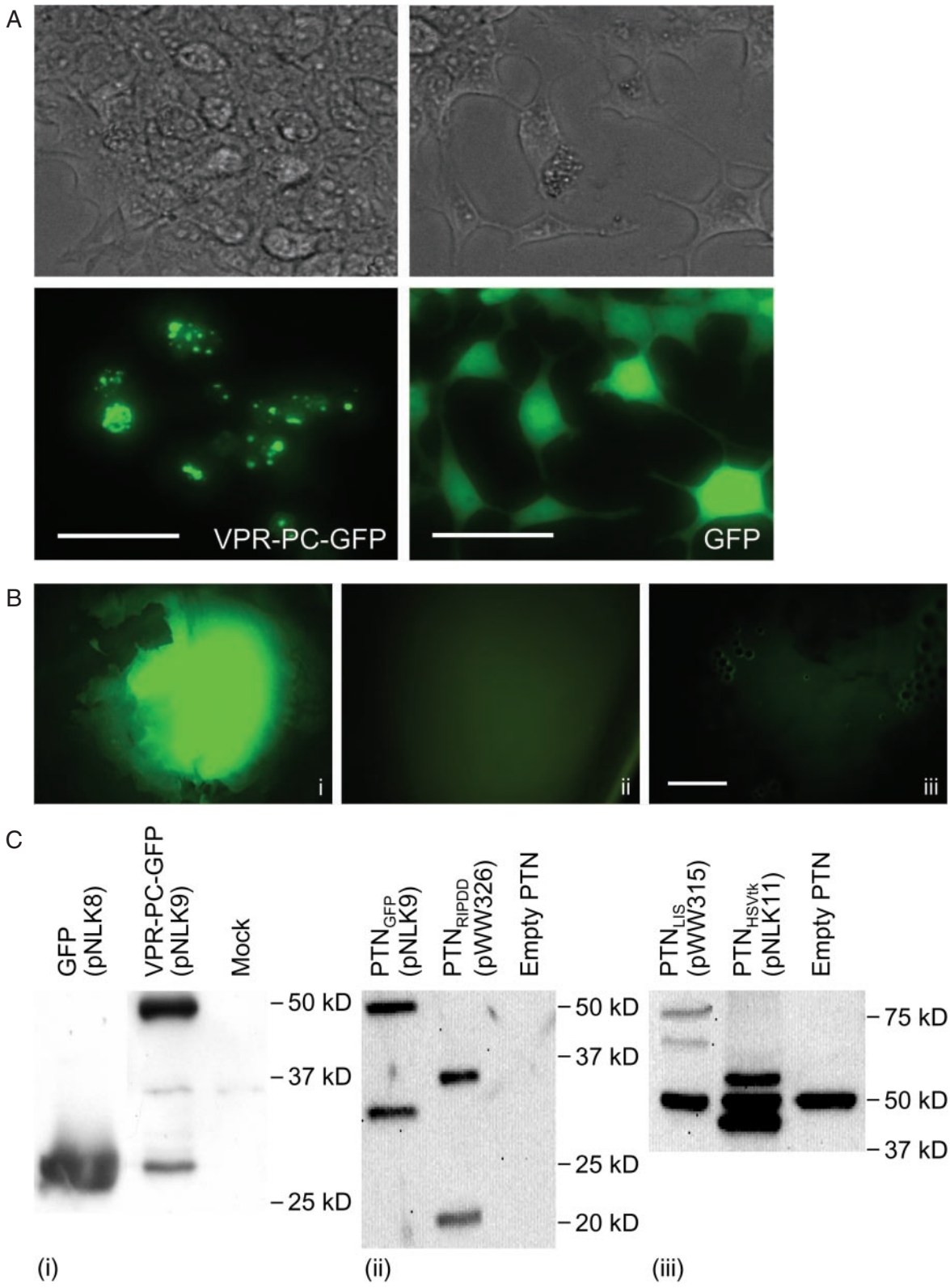

Figure 2. Localization and encapsidation of VPR-PC-tagged heterologous proteins in HEK293-T producing PTNs. (**A**) Intracellular distribution of VPR-PC-tagged and native GFP (scalebars 100 μm). (**B**) Fluorescence micrographs of pellets obtained by centrifugation of HEK293-T supernatants transfected with helper plasmids pWW203 and pLTR-G and (i) pNLK9 (P_{hEF1a}-VPR-PC-GFP-pA; 12 μg p24), (ii) pNLK8 (P_{hEF1a}-GFP-pA; 17 μg p24) or (iii) no additional vector, (12 μg p24) (scalebar 500 μm). (**C**) Western blot analysis of PTN-producing cell lysates (i) and HIS- (ii) or HA- (iii) tagged proteins in centrifugation-purified PTN preparations equally adjusted to 135 ng p24. VPR-linked as well as processed native proteins are visualized (GFP, 28 kDa; RIPDD, 16 kDa; *Herpes simplex* thymidine kinase [HSVtk], 37 kDa, Linamarase [Lis], 75 kDa). The 50 kDa signal in (iii) represents an unspecific interaction between a PTN protein and the HA tag-recognizing antibody.

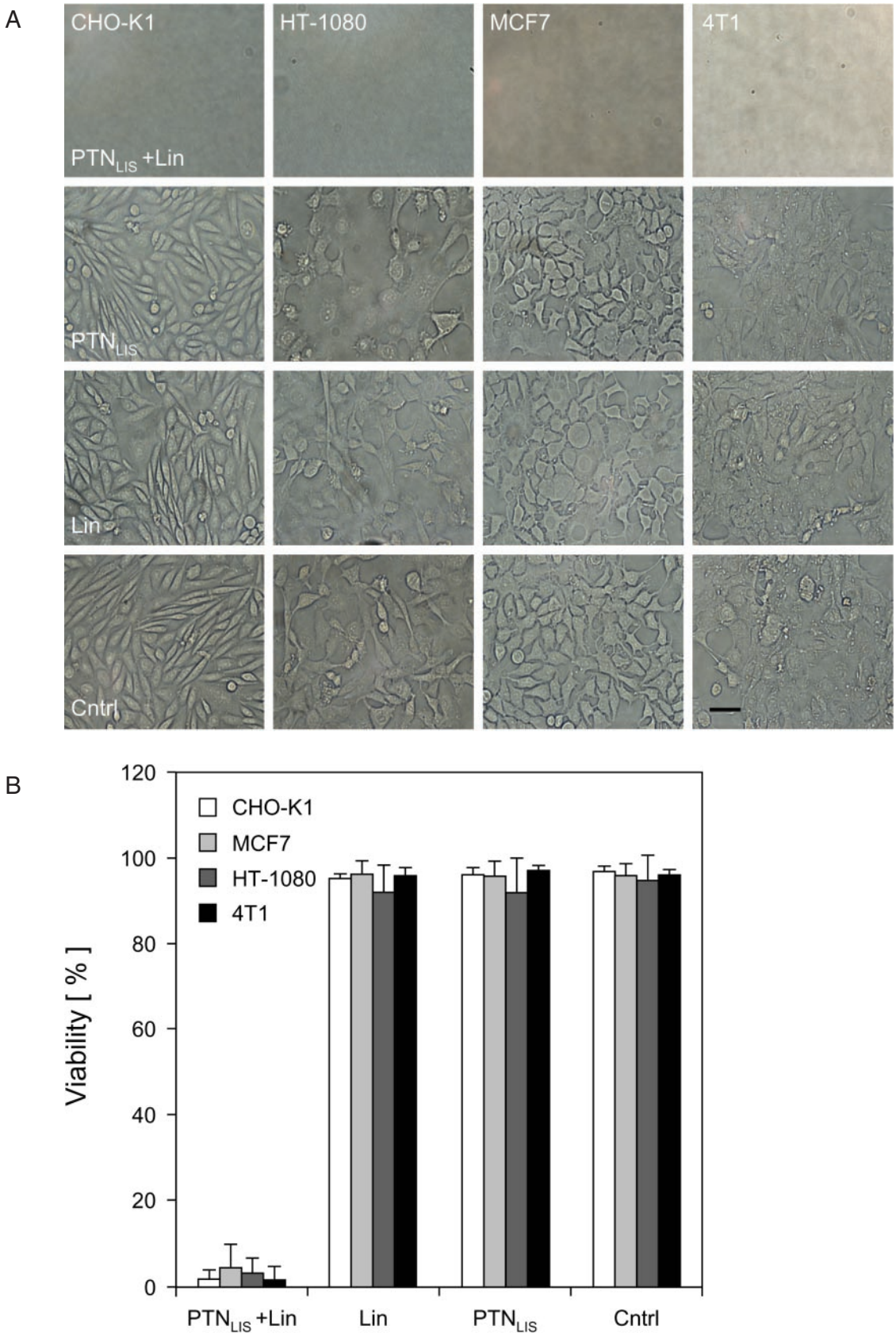

Figure 3. Impact of PTN-delivered linamarase-linamarin prodrug system on (tumor) cell viability 96 h after administration. (**A**) Light microscopy of monolayer cultures treated with (i) linamarase-transducing nanoparticles (PTN$_{LIS}$) and linamarin, (ii) PTN$_{LIS}$ only, (iii) linamarin only or (iv) empty control particles (scalebar 50 μm). (**B**) Viability of cells treated with PTN$_{LIS}$ and linamarin (Lin), Lin or PTN$_{LIS}$ alone or untreated as control (Cntrl).

(pNLK8) lacking specific addresses were homogeneously dispersed into the cytosol (Figure 2A). GFP-transducing nanoparticles were purified and concentrated by simple centrifugation from which the bright fluorescence of encapsidated GFP in particle pellets could be observed (Figure 2B). The lack of GFP signal in purified samples originating from co-production of particles and native GFP suggested that VPR-PC-GFP is indeed packaged by the viral mechanism rather than by an unspecific interaction with viral proteins (Figure 2B). Also, western blot analysis showed partially processed full-length VPR-PC-GFP fusion protein present in production cell lysates and processed native fluorescent GFP in purified PTNs (Figure 2C). Quantitative correlation of GFP fluorescence, western blot signal and lentivirion number indicated that 2200 ± 340 GFP molecules were packaged into each nanoparticle.

Validation of PTNs using prodrug systems

For PTN validation we focused on a drug-delivery system in which toxic proteins were packaged and delivered in an attempt to induce apoptosis in tumor cells. To that end, we targeted the 120 amino acid RIPDD into lentiviral nanoparticles (20). Although western blot analysis of pelleted particles confirmed successful packaging and processing of RIPDD (Figure 2C), it was difficult to isolate a sufficient number of RIPDD-transducing nanoparticles due to efficient RIPDD-triggered apoptosis in the producer cell line (data not shown). Due to this problem, the initial strategy of directly delivering apoptosis-triggering proteins was modified to a prodrug-drug system consisting of HSVtk-transducing nanoparticles which enable conversion of the prodrug ganciclovir into DNA replication-blocking nucleoside analogs (26). As expected, the transient packaging cell line was not impacted by VPR-PC-HSVtk. However, despite its accurate targeting to lentivirions (Figure 2C), effective killing of transduced and ganciclovir-treated tumor populations could not be observed, probably due to the lack of a bystander effect in this system (26) (data not shown).

In a second attempt to produce a viable (pro)drug system we successfully targeted the 75 kDa VPR-PC-LIS linamarase fusion protein into lentiviral nanoparticles (Figure 2C). Linamarase-transducing nanoparticles were stable for at least 48 h at room temperature as no cyanide production was detected when encapsidated linamarase was incubated with linamarin in a cell-free system (data not shown). However, co-application of linamarase-transducing nanoparticles with linamarin resulted in cyanide production and effective killing of rodent (CHO-K1, 4T1) and human (HT-1080, MCF7) (tumor) cell lines (Figure 3A). Administration of linamarin alone, or together with empty nanoparticles, did not adversely impact cell viability, and cyanide content was undetectable confirming that linamarase and lentivirions are non-toxic, that no detectable auto-decomposition of linamarin occurs and that the cells lack endogenous linamarase activity (Figure 3B). At non-limiting and non-toxic linamarin concentrations of 750 μg/ml, cyanide production was cell type-specific and showed a strong linear correlation between the number of particles administered and the observed cyanide concentration (Figure 4A). As exemplified in treated CHO-K1 monolayer cultures, linamarase-mediated cyanide

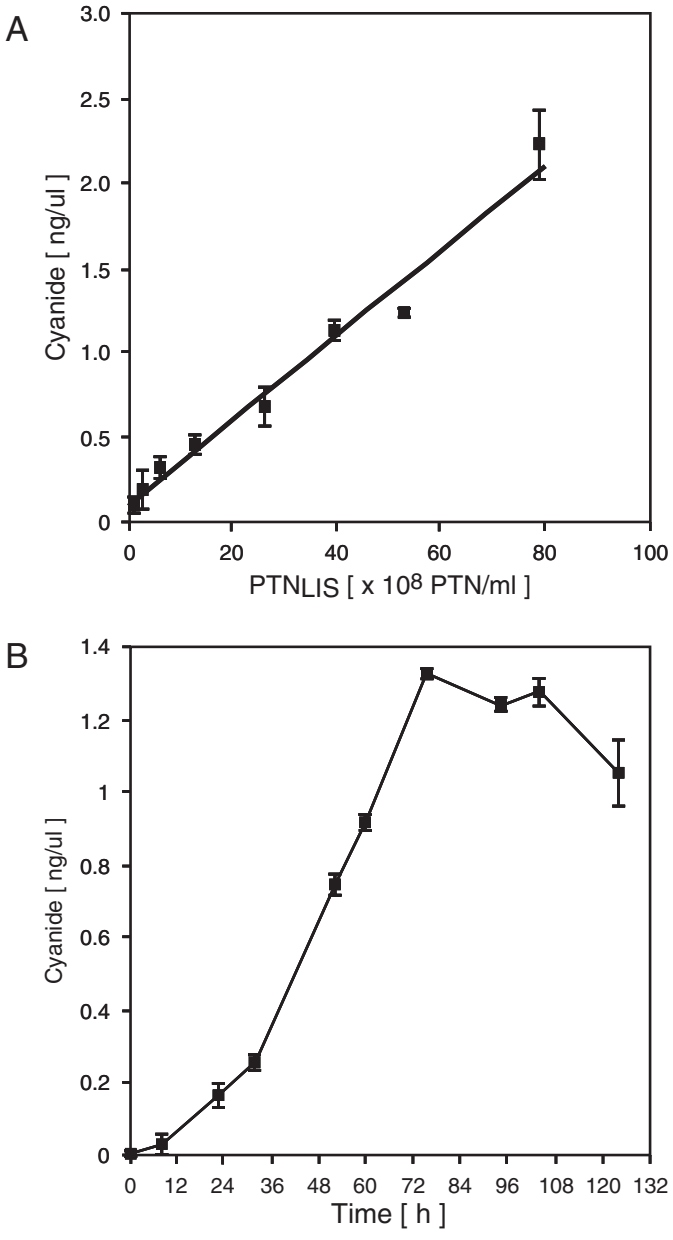

Figure 4. Cyanide production in CHO-K1 treated with a combination of linamarase-transducing nanoparticles (PTN_{LIS}) and linamarin. (**A**) Correlation of PTN_{LIS} number administered and the cyanide concentration produced in CHO-K1 cultures after 72 h. (**B**) Cyanide production kinetics in PTN_{LIS}-transduced CHO-K1 cultures (5×10^8 PTN's, 800 000 cells, 8 ml culture medium).

production steadily accumulated in the culture medium until cell killing was complete (Figures 3B and 4B; see movie in Supplementary data).

Impact of linamarase-transducing nanoparticles on tumor spheroids

Since results obtained with monolayer cultures may deviate from those generated in tissues, we produced MCF7- and 4T1-derived solid state tumor-mimicking microtissues and treated them with linamarase-transducing nanoparticles prior to administration of linamarin. Microscopic analysis

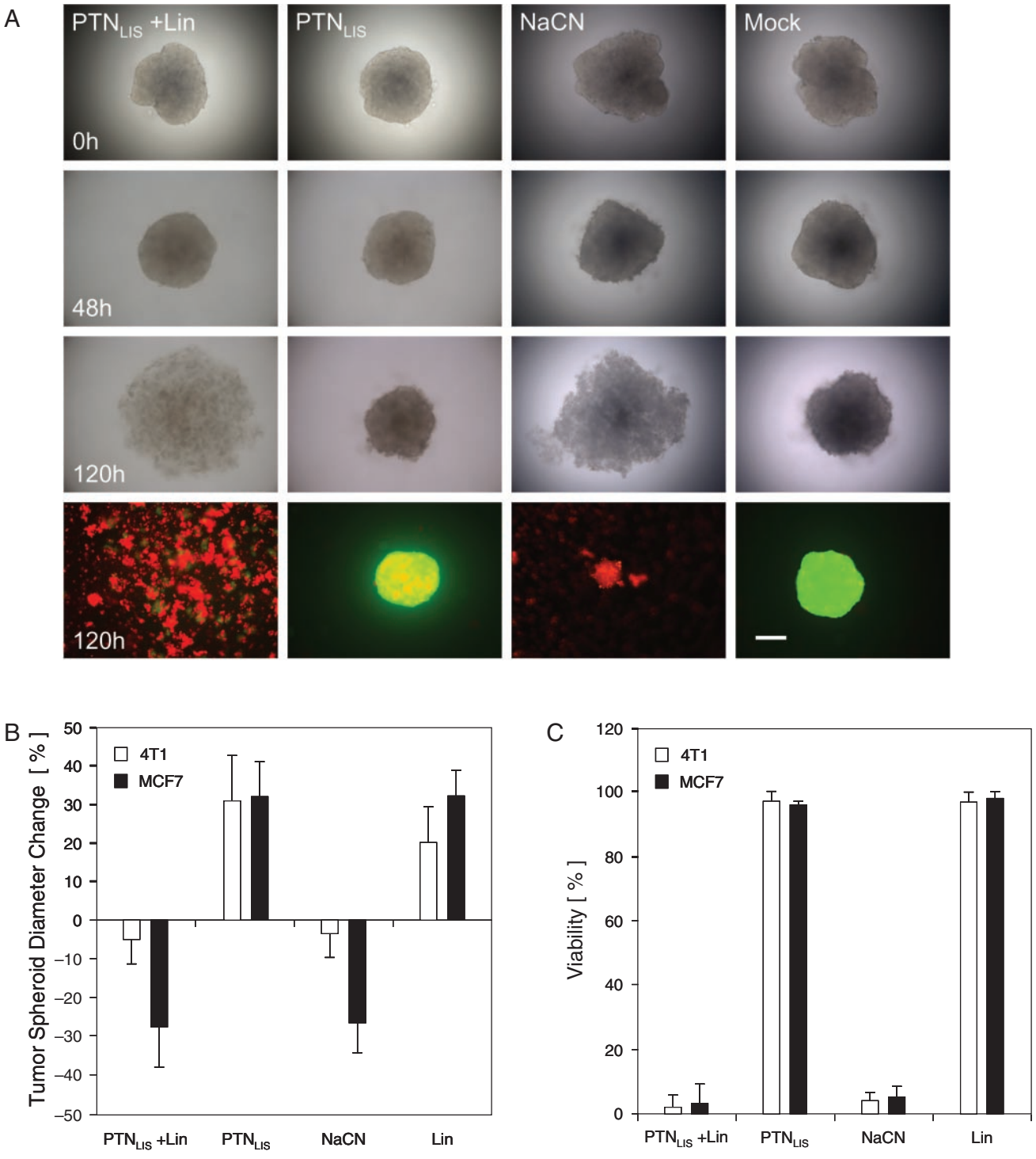

Figure 5. Impact of PTN-delivered linamarase-linamarin prodrug system on 4T1-derived tumor spheroids. (**A**) Light and fluorescence (ethidium bromide, dead cells shown in red; fluorescein-diacetate, viable cells shown in green) micrographs of 4T1-derived tumor spheroids treated up to 120 h with linamarase-transducing nanoparticles (PTN$_{LIS}$) plus linamarin, PTN$_{LIS}$ alone, NaCN or mock-transfected PTN production supernatants as control (Mock) (scalebar 200 μm). (**B** and **C**) Quantitative analysis of 4T1- and MCF7-derived tumor spheroid diameters changes (B) and viability (C) 120 h after administration of PTN$_{LIS}$/LIN, PTN$_{LIS}$, NaCN or linamarin as control (Lin).

of treated tumor spheroids showed significant reduction of the microtissues' diameter after 120 h and global red fluorescence after fluorescein-diacetate/ethidium bromide-based live/dead staining which confirms that massive cell death had occurred (Figure 5A and B; see also Figure 6). At 120 h, all tumor spheriods were disaggregated for viability assessment of individual cells which confirmed low cell viability in all cyanide-treated groups regardless of whether cyanide was directly applied or produced *in situ* by conversion of linamarin (Figure 5C).

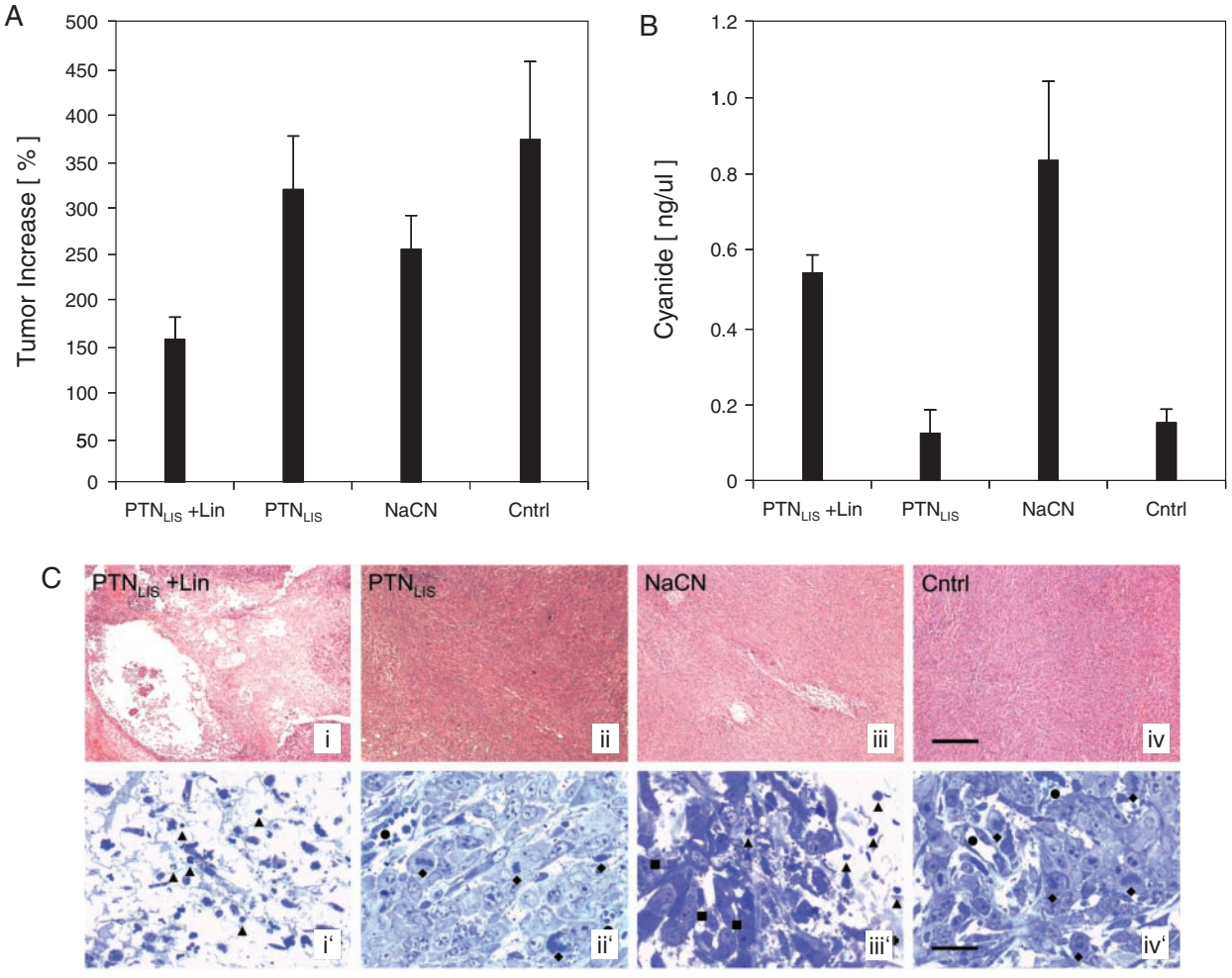

Figure 6. Tumor growth retardation in mice after administration of linamarin-transducing nanoparticles (PTN_{LIS}) and linamarin (Lin). (**A**) Size of 4T1 tumors and (**B**) serum cyanide levels of mice 4 days after injection of PTN_{LIS} and Lin, PTN_{LIS} alone, NaCN or Lin alone (Cntrl). (**C**) Histologic analysis of treated tumor explants using haematoxylin–eosin (i,ii,iii and iv; sections; scalebar 400 μm) and toluidine blue (i′,ii′,iii′ and iv′; semi-thin sections; scalebar 20 μm) staining revealing the effects of different treatment modalities versus control in 4T1 tumors. i and i′: Tumors treated by a combination of PTN_{LIS} and linamarin showed a large necrotic area around the application site. Black triangles indicate apoptotic figures and bodies at different stages of chromatin consolidation. ii and ii′: Treatment with PTN_{LIS} alone had practically no effect on the tumor growth. The blood vessels were preserved (black circles) and mitotic figures (black diamonds) were detectable close to the application site. iii and iii′: Sodium cyanide injection had a pronounced effect only locally at the site of application as indicated by apoptotic profiles (black triangles). At a distance lower than 250 μm of the application canal tumors exhibited normal cell morphology (black squares). iv and iv′: The tumor cells in the control group treated by Lin demonstrated typical mitotic activity (black diamonds) and normal blood vessels (black circles) were formed.

Functional linamarase transduction retards tumor progression in mice

The 4T1 cells, which are commonly used as a human breast cancer model in mice, were inoculated into nude mice to form solid tumors. At a diameter of around 6 mm, DMEM containing either (i) a mixture of linamarin (500 μg) and 1.5×10^{10} linamarase-transducing nanoparticles, (ii) linamarase-transducing nanoparticles only (1.5×10^{10}) or (iii) sodium cyanide (18 μg), were injected into the center of the tumor. Control mice received only linamarin injections. Mice were treated over 4 days after which blood samples were collected. Tumor sizes were measured again prior to surgical removal and blood serum samples were assessed for their cyanide concentration. Although cyanide traces could be detected in treated mice, which clearly indicated that cyanide injected or generated by the transduced (pro)drug system in the tumor was diffusing through the tissue into the blood system, the animals did not show any signs of nausea. Within 4 days, tumors treated with linamarase-transducing nanoparticles and linamarin or NaCN exhibited a significant decrease in tumor growth when compared to linamarin-treated control tumors (Figure 6A). In each group cyanide level was measured (Figure 6B) and a correlation between decrease in tumor growth and cyanide level was observed. Histologic analysis of tumor tissue explants showed large lesions around the injection site which was consistent with cyanide-mediated killing of both transduced and bystander cells. Increased lesions observed for *in situ*-produced cyanide likely resulted from constant high cyanide concentrations in the tumor (Figure 6C).

DISCUSSION

Protein pharmaceuticals enable transient dose-dependent therapeutic interventions in the absence of genomic

alterations, yet require sophisticated downstream processing and specific formulations for optimal pharmacokinetics (1). Viral gene therapy concepts which use advanced transgene delivery systems may offer long-term correction of genetic deficiencies, but expression dosing and random integration into target chromosomes remain major challenges (27). We have shown that PTNs could combine the best of both therapeutic strategies: (i) one-step transient production and packaging of native therapeutic proteins of up to 75 kDa using standard biopharmaceutical manufacturing technology, (ii) one-step purification and concentration of encapsidated proteins by simple centrifugation and (iii) cytosolic protein delivery without transduction of genetic information. Also, the particle tropism could be modified for tissue-specific delivery by pseudotyping (28) and PTNs may show improved pharmacokinetics as the protein therapeutic is protected from degradation *en route* to the target site. As demonstrated by the production and functional delivery of the Cassava prodrug system to eliminate tumor cells both *in vitro* and *in vivo*, generic protein transduction systems have the potential to provide affordable, safe and efficient medicines in the not-too-distant future.

SUPPLEMENTARY DATA

Supplementary Data are available at NAR Online.

ACKNOWLEDGEMENTS

The authors thank Manuel Izquierdo for providing pLlisSP, Thomas M. Fletcher for pLR2P-R-PC-IN, Pasquale Vito for pRIPDD and Valérie Frascogna and Monique Stanciu for excellent technical assistance. This work was supported by the Swiss National Science Foundation (grant no. 631-065946), the Swiss State Secretariat for Education and Research within EC Framework 6 and Cistronics Cell Technology GmbH, Einsteinstrasse 1-5, CH-8093 Zurich, Switzerland. Funding to pay the Open Access publication charges for this article was provided by ETH Zurich.

Conflict of interest statement. None declared.

REFERENCES

1. Wurm,F.M. (2004) Production of recombinant protein therapeutics in cultivated mammalian cells. *Nat. Biotechnol.*, **22**, 1393–1398.
2. Cavazzana-Calvo,M., Thrasher,A. and Mavilio,F. (2004) The future of gene therapy. *Nature*, **427**, 779–781.
3. Naldini,L., Blomer,U., Gage,F.H., Trono,D. and Verma,I.M. (1996) Efficient transfer, integration, and sustained long-term expression of the transgene in adult rat brains injected with a lentiviral vector. *Proc. Natl Acad. Sci. USA*, **93**, 11382–11388.
4. Weber,W., Rimann,M., Spielmann,M., Keller,B., Daoud-El Baba,M., Aubel,D., Weber,C.C. and Fussenegger,M. (2004) Gas-inducible transgene expression in mammalian cells and mice. *Nat. Biotechnol.*, **22**, 1440–1444.
5. Bushman,F.D. (2003) Targeting survival: integration site selection by retroviruses and LTR-retrotransposons. *Cell*, **115**, 135–138.
6. Fischer,A., Hacein-Bey-Abina,S. and Cavazzana-Calvo,M. (2004) Gene therapy of children with X-linked severe combined immune deficiency: efficiency and complications. *Med. Sci. (Paris)*, **20**, 115–117.
7. Fletcher,T.M.,III, Soares,M.A., McPhearson,S., Hui,H., Wiskerchen,M., Muesing,M.A., Shaw,G.M., Leavitt,A.D., Boeke,J.D. and Hahn,B.H. (1997) Complementation of integrase function in HIV-1 virions. *EMBO J.*, **16**, 5123–5138.
8. Langer,R. (1998) Drug delivery and targeting. *Nature*, **392**, 5–10.
9. Pack,D.W., Hoffman,A.S., Pun,S. and Stayton,P.S. (2005) Design and development of polymers for gene delivery. *Nature Rev. Drug Discov.*, **4**, 581–593.
10. Glover,D.J., Lipps,H.J. and Jans,D.A. (2005) Towards safe, non-viral therapeutic gene expression in humans. *Nature Rev. Genet.*, **6**, 299–310.
11. Wadia,J.S. and Dowdy,S.F. (2002) Protein transduction technology. *Curr. Opin. Biotechnol.*, **13**, 52–56.
12. Weigelt,B., Peterse,J.L. and van 't Veer,L.J. (2005) Breast cancer metastasis: markers and models. *Nature Rev. Cancer*, **5**, 591–602.
13. Culver,K.W., Ram,Z., Wallbridge,S., Ishii,H., Oldfield,E.H. and Blaese,R.M. (1992) *In vivo* gene transfer with retroviral vector-producer cells for treatment of experimental brain tumors. *Science*, **256**, 1550–1552.
14. Riis,L., Bellotti,A.C., Bonierbale,M. and O'Brien,G.M. (2003) Cyanogenic potential in cassava and its influence on a generalist insect herbivore *Cyrtomenus bergi* (Hemiptera: Cydnidae). *J. Econ. Entomol.*, **96**, 1905–1914.
15. Prabhakaran,K., Li,L., Borowitz,J.L. and Isom,G.E. (2004) Caspase inhibition switches the mode of cell death induced by cyanide by enhancing reactive oxygen species generation and PARP-1 activation. *Toxicol. Appl. Pharmacol.*, **195**, 194–202.
16. Kousparou,C.A., Epenetos,A.A. and Deonarain,M.P. (2002) Antibody-guided enzyme therapy of cancer producing cyanide results in necrosis of targeted cells. *Int. J. Cancer*, **99**, 138–148.
17. Cortes,M.L., de Felipe,P., Martin,V., Hughes,M.A. and Izquierdo,M. (1998) Successful use of a plant gene in the treatment of cancer *in vivo*. *Gene. Ther.*, **5**, 1499–1507.
18. Mochizuki,H., Schwartz,J.P., Tanaka,K., Brady,R.O. and Reiser,J. (1998) High-titer human immunodeficiency virus type 1-based vector systems for gene delivery into nondividing cells. *J. Virol.*, **72**, 8873–8883.
19. Cortes,M.L., Garcia-Escudero,V., Hughes,M. and Izquierdo,M. (2002) Cyanide bystander effect of the linamarase/linamarin killer-suicide gene therapy system. *J. Gene. Med.*, **4**, 407–414.
20. Boorsma,M., Nieba,L., Koller,D., Bachmann,M.F., Bailey,J.E. and Renner,W.A. (2000) A temperature-regulated replicon-based DNA expression system. *Nat. Biotechnol.*, **18**, 429–432.
21. Mitta,B., Rimann,M., Ehrengruber,M.U., Ehrbar,M., Djonov,V., Kelm,J. and Fussenegger,M. (2002) Advanced modular self-inactivating lentiviral expression vectors for multigene interventions in mammalian cells and *in vivo* transduction. *Nucleic Acids Res.*, **30**, e113.
22. Kelm,J.M., Timmins,N.E., Brown,C.J., Fussenegger,M. and Nielsen,L.K. (2003) Method for generation of homogeneous multicellular tumor spheroids applicable to a wide variety of cell types. *Biotechnol. Bioeng.*, **83**, 173–180.
23. Mitta,B., Rimann,M. and Fussenegger,M. (2005) Detailed design and comparative analysis of protocols for optimized production of high-performance HIV-1-derived lentiviral particles. *Metab. Eng.*, **7**, 426–436.
24. Layne,S.P., Merges,M.J., Dembo,M., Spouge,J.L., Conley,S.R., Moore,J.P., Raina,J.L., Renz,H., Gelderblom,H.R. and Nara,P.L. (1992) Factors underlying spontaneous inactivation and susceptibility to neutralization of human immunodeficiency virus. *Virology*, **189**, 695–714.
25. Huang,M.B., Khan,M., Garcia-Barrio,M., Powell,M. and Bond,V.C. (2001) Apoptotic effects in primary human umbilical vein endothelial cell cultures caused by exposure to virion-associated and cell membrane-associated HIV-1 gp120. *J. Acquir. Immune Defic. Syndr.*, **27**, 213–221.
26. Gentry,B.G., Im,M., Boucher,P.D., Ruch,R.J. and Shewach,D.S. (2005) GCV phosphates are transferred between HeLa cells despite lack of bystander cytotoxicity. *Gene. Ther.*, **12**, 1033–1041.
27. Cavazzana-Calvo,M., Hacein-Bey-Abina,S. and Fischer,A. (2002) Gene therapy of X-linked severe combined immunodeficiency. *Curr. Opin. Allergy. Clin. Immunol.*, **2**, 507–509.
28. Liu,S.L., Halbert,C.L. and Miller,A.D. (2004) Jaagsiekte sheep retrovirus envelope efficiently pseudotypes human immunodeficiency virus type 1-based lentiviral vectors. *J. Virol.*, **78**, 2642–2647.